



# Synthesis of locust bean gum-based terpolymer bentonite composite: evaluation for indigo carmine adsorption

Sirajo Abubakar Zauro, Vishalakshi Badalamoole \*

Department of Post-Graduate Studies and Research in Chemistry, Mangalore University,  
Mangalagangothri, 574199 (DK), Karnataka, India

\*Corresponding author E-mail: [vishalakshi2009@yahoo.com](mailto:vishalakshi2009@yahoo.com)

## Abstract

A terpolymer gel composite is made up of locust bean gum (LBG), diallyldimethylammonium chloride (DADMAC), 2-acrylamido-2-methyl-1-propane sulfonic acid (AMPS) and bentonite (BNT) was prepared using methylenebisacrylamide (MBA) as crosslinker via microwave irradiation and characterized using FTIR, TGA and SEM techniques. Swelling behavior of the composite was studied under different pH conditions. The composite was also evaluated for adsorption of anionic dye 'Indigo Carmine' (IC). The behaviour of the composite was compared with the terpolymer gel without the clay component. The gel showed remarkably higher swelling under neutral pH compared to the composite. The adsorption capacity of the terpolymer gel without clay for Indigo Carmine dye is also found to be higher (17.36 mg/g) compared to the clay composite (11.99 mg/g). The adsorption data were subjected to three different isotherm models namely; Freundlich, Langmuir and Temkin and were observed to be explained best by Freundlich model. The adsorption of indigo Carmine on the terpolymer gel and the composite is observed to be a second order kinetic process.

**Keywords:** Adsorption; Bentonite; Diallyldimethylammonium chloride; Indigo carmine; Locust bean gum; 2-acrylamido-2-methyl-1-propane sulfonic Acid.

## 1. Introduction

The demand for manufactured goods across the globe results in the use of synthetic products such as dyes in various industries (textile, leather, paper, rubber, plastic, cosmetic etc). This has led to the proportionate release of a large quantity of effluent containing non-biodegradable, toxic and carcinogenic colored substances into the environment. The presence of this colored pollutants becomes increasingly a major threat to water bodies and their removal from waste water by means of an environmentally friendly technique is a major challenge (Malana, et al, 2010; Zhou, et al, 2014; Karthika and Vishalakshi, 2015; Gan, et al, 2015; Fossonkankeu, et al, 2015). Several physico-chemical methods such as chemical precipitation, ion exchange, membrane separation, chemical reduction, chemical oxidation, advanced oxidation processes (Santos and Boaventura, 2016) have been employed in the removal of toxic substances from the environment. But, the efficiency of these methods to remove the dye molecules are still low and the methods are time consuming, expensive and sometimes generate large amount of sludge which are toxic to the living organisms in the environment. Hence, adsorption using composite based biopolymers has been described as one of the most effective and promising technique for removal of such pollutants (Mahida and Patel 2016; Maity and Ray 2016; Robati, et al, 2016).

The composites of polymer-clay have been gaining increased attention by researchers globally due to the hybrid properties they exhibit when compared with either the polymer or clay separately. A wide range of polymer-clay composite has been produced and used for water treatment (Sebastian, et al, 2014; Gupta, et al,

2016), dye adsorption (El Haddad, et al, 2012; Patil and Shrivastava, 2015) etc.

The synthesis of ionic copolymers has been gaining significant interest among researchers (Tirelli and Hunkeler, 1999). Diallyldimethylammonium chloride (DADMAC) is one of the water soluble cationic monomer that has wide range of applications in water treatment, medicine, electrical switches, etc. (Jing and Hongfei, 2001; Zhao, et al, 2010). Similarly, 2-acrylamido-2-methylpropane sulfonic acid sodium salt (AMPS) as an anionic monomer has received attention due to its strongly ionizable sulfonate group (Durmaz and Okay, 2000). Biopolymers functionalized with ionic molecules with DMDMAC and AMPS can be potential adsorbents for removal of ionic dyes from effluents.

Indigo carmine is one of the most widely used synthetic dyes in fiber industries for dyeing wool and silk. It has also been used as dermatological agent, biological stain, antibacterial agent and additive to poultry feed (Ramesh and Sreenivasa, 2015). Despite its potential applications in the textile and leather industries, the IC dye is considered as potent carcinogen, recalcitrant and toxic to mammalian cells (Gopi, et al, 2017).

There are many reports on removal of IC using different adsorbents. The removal of IC from aqueous solution using cross linked Chitosan was reported (Cestari, et al, 2008). The preparation of a polyampholyte nanocomposite hydrogels made up of acrylic acid (AA), 2-(diethylamino)ethyl methacrylate (2-DEAEMA) and montmorillonite (MMT) and its potentials for Indigo Carmine removal from aqueous solution was reported (Dalaran, et al, 2011). Geyikçi, (2016), reported the adsorption of IC onto montmorillonite using factorial design. The removal of IC dye using



Chitin nanowhisker (ChNW)-functionalized electrospun PVDF membrane was reported and the maximum adsorption of 72.6 mg/g was recorded (Gopi, et al, 2017). In our previous work, we have reported the adsorption of IC dye on LBG-g-PDADMAC (Zauro and Vishalakshi, 2016).

A thorough survey of literature indicated that the information for the adsorption of IC dye on biopolymer based clay composite is limited. Hence preparation of a terpolymer gel LBG-g-poly(DADMAC-co-AMPS) and its composite with bentonite (BNT), LBG-g-poly(DADMAC-co-AMPS)/BNT has been attempted to be used as a potential adsorbents for the dye, IC. The effect of incorporation of clay in the gel material on the adsorption behavior has been studied in detail.

## 2. Materials and methods

### 2.1. Materials

Locust bean gum (LBG), Diallyldimethylammonium chloride (DADMAC), 2-acrylamido-2-methyl propane sulfonic acid (AMPS) were purchased from Sigma Aldrich Chemical Company, India, Potassium chloride, HCl, Disodium hydrogen phosphate, Sodium chloride were obtained from Merck Ltd Mumbai, India. Ammonium peroxodisulphate (APS) and N, N-methylene-bis-acrylamide (MBA) were obtained from SpectroChem Pvt. Ltd Mumbai, India. Indigo Carmine dye (IC) was obtained from s. d. fine chemicals Ltd. Mumbai, India. Acetone was obtained from Nice Chemicals pvt Ltd., Kerala, India. Methanol was obtained from Himedia Laboratories Pvt, Ltd., Mumbai, India. All the reagents were used as obtained. Throughout the experiments distilled water was used.

### 2.2. Methods

#### 2.2.1. Preparation of LBG-g-poly(DADMAC-co-AMPS) gel

The grafting of poly(DADMAC-co-AMPS) on to LBG was carried out based on the reported literature (Kaity, et al, 2013). A fixed amount of LBG (0.1g) was dispersed in 20ml distilled water and stirred overnight followed by addition of APS (0.008) and stirred for an hour. Specified amount of DADMAC (0.15-0.40g) and AMPS (0.1-0.30g) were added to the above solutions followed by MBA (0.005g) and stirred for 8 hours. The solution was then irradiated in a domestic microwave (LG-Gril-Intellowave, India) at 80 watt for 120 seconds with alternate heating and cooling. The solution was then left overnight at ambient temperature to complete grafting and precipitated out using acetone. The precipitate was separated and washed with methanol 2-3 times to remove the un-reacted monomers. The grafted gum was dried in a hot air oven overnight at 50°C. All weight measurements were carried out using a digital weighing balance (SHIMADZU AUX 120, Japan) with an accuracy of  $\pm 0.1$ mg. The percentage grafting (GP) and grafting efficiency (GE) were calculated using the below equations;

$$GP(\%) = \frac{W_1 - W_0}{W_0} \times 100 \quad (1)$$

$$GE(\%) = \frac{W_1 - W_0}{W_2} \times 100 \quad (2)$$

Where,  $W_0$ ,  $W_1$  and  $W_2$  are the weight of LBG, grafted gel and total amount of monomers taken for grafting process respectively.

#### 2.2.2. Preparation of LBG-g-poly(DADMAC-co-AMPS) gel/BNT

The LBG-g-poly(DADMAC-co-AMPS)/BNT composite gel was made following same procedure as in 2.2.1 above but with addition of BNT (0.01-0.03g) under continuous stirring after addition

of monomers but prior to microwave irradiation. The GP (%) and GE (%) were calculated using equations 1 and 2 respectively.

### 2.3. Characterization

LBG, LBG-g-poly(DADMAC-co-AMPS) and LBG-g-poly(DADMAC-co-AMPS)/BNT were characterized using FTIR spectrophotometer (Prestige-21, Shimadzu, Japan). The FTIR spectra were recorded in the wave number range of 4000 to 400  $\text{cm}^{-1}$  during 40 scans, with resolution of 2  $\text{cm}^{-1}$ . The thermogravimetric analysis of the samples were achieved by heating between the temperature ranges of 10-700 °C, under nitrogen atmosphere at 10°C/min using DSC-TGA (Q600 V20.9 model) Japan. The SEM images were recorded after gold sputtering of the samples in order to make them electrically conductive and scanned at 20 KVA using and JEOL JSM-6380LA (USA) scanning electron microscope.

### 2.4. Swelling study

A solution of 0.2M KCl and 0.2M HCl was prepared in order to obtain a buffer of pH 1.2. Similarly, 0.1M solution of  $\text{Na}_2\text{HPO}_4$  and 0.1M NaCl were also prepared for the preparation of buffer of pH 7.0 and pH 9.0 by dissolving appropriate amount of the chemicals in distilled water (Mithun and Vishalakshi, 2014) and the pH were measured using a digital pH meter (335, Systronics, India). A known amount (g) of the grafted gel/composite samples were weighed ( $W_0$ ) accurately and immersed in a solution of different pH (1.2, 7.0 and 9.0) and at different time intervals the samples were removed and wiped by blotting with tissue paper and re-weighed ( $W_1$ ) and the process was repeated until an equilibrium was reached (Shukla, et al, 2012). The swelling ratio (SR) in g/g was calculated from the relation below:

$$SR = \frac{W_1 - W_0}{W_0} \quad (3)$$

### 2.5. Dye adsorption study

The adsorption study was carried out in a solution of 100 mg/L of IC solution with known amount of LBG-g-poly(DADMAC-co-AMPS) and LBG-g-poly(DADMAC-co-AMPS)/BNT. The gel and composite samples were immersed in the dye solution and at different time interval 1mL of the solution was withdrawn and diluted appropriately and the absorbance was measured using UV-visible spectrophotometer (UV-1800 SHIMADZU, Japan) at  $\lambda_{\text{max}}$  of 610 nm. Predetermined calibration curves were used to convert the absorbance values into concentration. Equilibrium adsorption studies were also carried out using different dye concentrations (10-100 mg/L). The amount of dye adsorbed at time  $t$  and at equilibrium was calculated from the equations 4 and 5 respectively.

$$q_t = \frac{(C_0 - C_t)}{M} \times v \quad (4)$$

$$q_e = \frac{(C_0 - C_e)}{M} \times v \quad (5)$$

Where  $q_t$  and  $q_e$  are the amount of dye adsorbed (mg/g) at time  $t$  and at equilibrium respectively.  $C_0$ ,  $C_t$  and  $C_e$  are dye concentrations (mg/L) at time  $t = 0$ ,  $t = t$  and at equilibrium respectively.  $M$  is the weight of the samples (g) and  $v$  is the volume (L) of the dye solution used for adsorption.

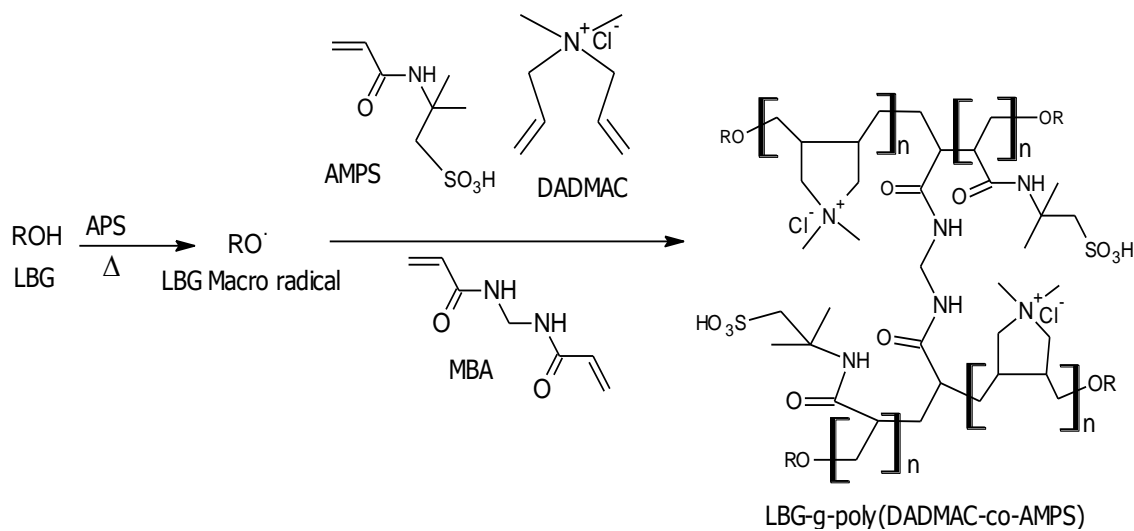
## 3. Results and discussion

### 3.1. Synthesis of LBG-g-poly(DADMAC-co-AMPS)

The mechanism of formation of LBG-g-poly(DADMAC-co-AMPS) is shown in Scheme 1. The initiator APS under microwave heating generates radicals that attack the LBG and abstract the hydrogen radicals thereby creating radical sites on LBG mole-

cules (macroradicals). During the polymerization process, grafting of the copolymer consisting of repeating units of AMPS and DADMAC occurs on LBG macroradicals. The presence of the bifunctional MBA in the copolymer chain results in formation of a

gel network of LBG-g-poly(DADMAC-co-AMPS). The presence of BNT during the polymerization process leads to the formation of clay entrapped LBG-g-poly(DADMAC-co-AMP gel composite.



**Scheme 1:** Proposed Scheme for the Formation of LBG-g-poly (DADMA-co-AMPS).

### 3.2. Optimization experiment

The grafting conditions were optimized by varying the DADMAC and AMPS content and the calculated values of GP (%) and GE (%) are presented in Table 1. The GE (%) increases as the AMPS content increases from 0.1 to 0.25g but decrease with increasing the AMPS to 0.30g keeping DADMAC content at 0.15g, whereas, the GP (%) increase and then decrease with further increase in the AMPS content. Similar trend was observed as the DADMAC content kept at 0.25g. However, as the DADMAC content was kept at 0.20g and varying the AMPS content from 0.15g to 0.25, the results showed a corresponding increase in both GP and GE. Further increase in AMPS to 0.30g results in decrease in the grafting parameters. The optimum condition for the formation of LBG-g-poly(DADMAC-co-AMPS) were found to be 0.20g DADMAC, 0.25g AMPS. The decrease in grafting parameters observed at higher DADMAC and AMPS contents is attributed to the formation of homopolymers in the reaction mixture (Giri, et al, 2015).

**Table 1:** Composition of Terpolymer gels/composite [LBG-G-Poly (DADMAC-Co-AMPS)] and their Grafting parameters (%) (APS =0.008g, MBA =0.005g)

LBG (g)	DADMAC (g)	AMPS(g)	BNT (g)	GP (%)	GE (%)
0.1	0.15	0.1	0.0	32.04	40.92
0.1	0.15	0.20	0.0	39.44	48.13
0.1	0.15	0.25	0.0	38.18	51.36
0.1	0.15	0.30	0.0	37.64	42.30
0.1	0.20	0.15	0.0	43.26	71.76
0.1	0.20	0.20	0.0	50.31	72.08
0.1	0.20	0.25	0.0	54.55	80.12
0.1	0.20	0.30	0.0	52.76	70.36
0.1	0.25	0.15	0.0	37.02	50.19
0.1	0.25	0.20	0.0	39.50	58.00
0.1	0.25	0.25	0.0	40.13	51.76
0.1	0.25	0.30	0.0	37.49	49.67
0.1	0.30	0.15	0.0	36.65	52.56
0.1	0.30	0.20	0.0	29.76	40.98
0.1	0.30	0.25	0.0	32.87	50.36
0.1	0.35	0.10	0.0	33.25	47.73
0.1	0.40	0.10	0.0	32.37	36.89
0.1	0.35	0.15	0.0	37.64	42.30
0.1	0.30	0.20	0.0	29.76	40.98
0.1	0.20	0.25	0.01	45.98	69.34
0.1	0.20	0.25	0.02	48.12	64.91
0.1	0.20	0.25	0.03	50.21	59.32

### 3.3. Characterization

#### 3.3.1. FTIR spectroscopy

The FTIR spectra of LBG, LBG-g-poly(DADMAC-co-AMPS) and LBG-g-poly(DADMAC-co-AMPS)/BNT are presented in Fig. 1. The LBG spectrum (Fig 1a) showed a broad band at 3350  $\text{cm}^{-1}$  which is attributed to O-H stretching. The peak at 2910  $\text{cm}^{-1}$  is assigned to C-H stretching. The peaks observed at 1010  $\text{cm}^{-1}$  is due to C-OH stretching. The peaks at 1190 and 1050  $\text{cm}^{-1}$  are for C-O-C stretching from glycosidic linkages. For LBG-g-poly(DADMAC-co-AMPS) (Fig 1b), in addition to the peaks observed in Fig. 1a, peaks at 1535  $\text{cm}^{-1}$  and 1720 were observed due to N-H bending and C=O stretching respectively. In the spectrum of LBG-g-poly(DADMAC-co-AMPS)/BNT shown in Fig 1c, there is a shift in C=O stretching vibration from 1720 to 1649  $\text{cm}^{-1}$  and additional occurrence of new peaks at 1017, 939 and 808  $\text{cm}^{-1}$  for Si-O-Si stretching, Si-O-Al bending and Si-O-C stretching respectively which provides evidence for incorporating BNT into the system.

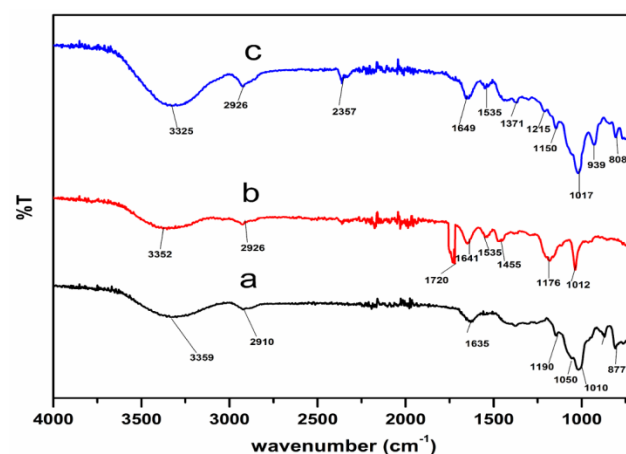


**Fig. 1:** FTIR Spectra of; a) LBG, b) LBG-g-poly(DADMAC-co-AMPS) and c) LBG-g-poly(DADMAC-co-AMPS)/BNT.

#### 3.3.2. TGA analysis

The TGA curves for LBG, LBG-g-poly(DADMAC-co-AMPS) and LBG-g-poly(DADMAC-co-AMPS)/BNT are presented in

Fig. 2. Fig. 2a shows three degradation steps for LBG. The 12% weight loss observed between 60-100 °C is attributed to the loss of adsorbed and structural. Between 284-320 °C the major weight loss of 40% was observed and is due to breakage of the glycosidic linkage in LBG. At 500°C the final decomposition of the gum occurs. The thermogram of LBG-g-poly(DADMAC-co-AMPS) (Fig. 2b), four decomposition stages were observed, with the major weight loss of 41% in the temperature range of 300-350 °C which is attributed to the breaking of the grafted chain on LBG. The final decomposition of the copolymer gel occurred between 510-600 °C and no residual mass was left 635 °C. For LBG-g-poly(DADMAC-co-AMPS)/BNT (Fig. 2c), several decomposition stages were observed. The first stage was the elimination of water molecule from the composite gel in the range of 60-141 °C. The final degradation occurred between 560- 660 °C leaving around 7% as residual matter, confirming the presence of clay particles in the gel-composite.

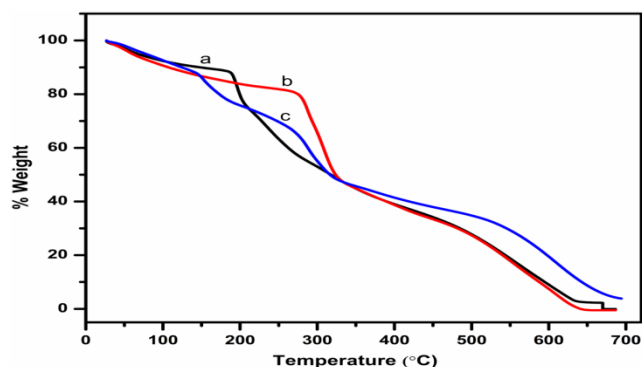


Fig. 2: Thermograms of; a) LBG, b) LBG-g-poly(DADMAC-co-AMPS) and c) LBG-g-poly(DADMAC-co-AMPS)/BNT.

### 3.3.3. SEM analysis

The surface morphology of LBG, LBG-g-poly(DADMAC-co-AMPS) and LBG-g-poly(DADMAC-co-AMPS)/BNT samples are presented in Fig. 3. The smooth, porous inhomogeneous surface structure of LBG (Fig. 3a) undergoes significant change on gel formation. The LBG-g-PDADMAC-co-AMPS (Fig 3b) appears cotton-like and irregular. The incorporation of BNT into the system produces a coarse and undulant surface with higher porosity compared to the LBG and LBG-g-poly(DADMAC-co-AMPS).

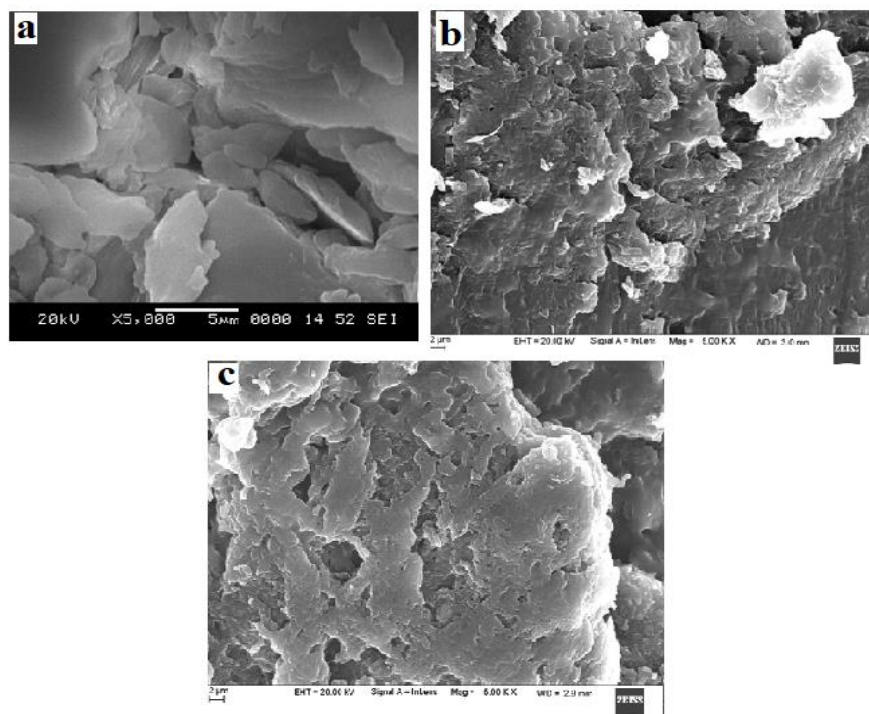


Fig. 3: SEM Images of; a) LBG, b) LBG-g-poly(DADMAC-co-AMPS) and c) LBG-g-poly(DADMAC-co-AMPS)/BNT.

### 3.4. Swelling studies

The swelling behavior of LBG-g-poly(DADMAC-co-AMPS) and LBG-g-poly(DADMAC-co-AMPS)/BNT in media of different pH is shown in figure 4a. The swelling of the gel is observed to be strongly affected by the pH, due to the presence of ionizable groups in the structure of these samples. (Bueno, et al, 2013). Swelling increases with increase in pH from 1.2 to 7.0 and decreases at higher pH conditions. At the pH of 7.0, there exist maximum numbers of ionic groups in the gel resulting in highest

swelling. Furthermore, at pH 9.0, the un-reacted hydroxyl groups of the LBG molecules and amine groups of both the MBA and AMPS are also deprotonated thereby decreasing the electrostatic repulsion and subsequently result in the decrease in SR (Ganji, et al, 2010). No significant swellings was observed at pH 1.2, as the sulfonate group of AMPS in both the gel and its composite remains protonated and exert insignificant electrostatic repulsive force.

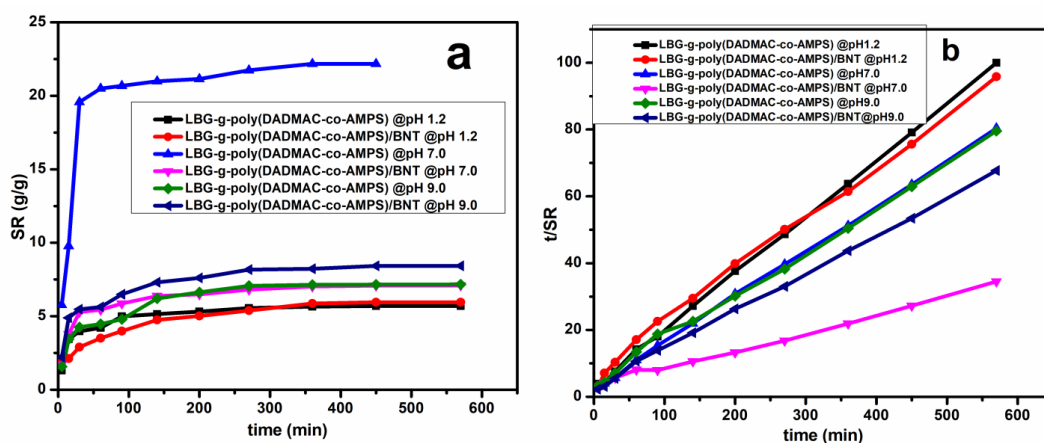


Fig. 4: a. Swelling data at different pH, b. Pseudo second order kinetic model fit.

### 3.4.1. Swelling kinetics

The swelling studies for the gel and the composite samples were carried out based on the standard methods reported in the literature (Martínez-Ruvalcaba, et al, 2009). The swelling mechanism of the gel/composite was determined by employing pseudo second-order kinetic model. The second-order kinetic equation is represented as equation 6 below;

$$\frac{t}{SR} = \frac{1}{k_2 S_{eq}^2} + \frac{1}{S_{eq}} t \quad (6)$$

Where,  $k_2$  and  $S_{eq}$  are the swelling rate constant and the equilibrium swelling ratio respectively. The value of  $R_i$ , the initial swelling rate is obtained as  $k_2 S_{eq}^2$ . The plot of  $t/SR$  vs  $t$  (Fig. 4b) is linear with a slope of  $1/S_{eq}$  and intercept of  $\frac{1}{k_2 S_{eq}^2}$ . This indicates that the swelling process is of second-order kinetics. The swelling parameters such as; swelling equilibrium ( $S_{eq}$ ) in g/g, swelling rate constant ( $k_2$ ) in g of water per gram of the adsorbent per minute and initial swelling rate ( $R_i$ ) were calculated using the swelling data obtained from the plot shown in Fig. 4b. Furthermore, the value of  $S_{eq}$  calculated from the slopes are in good agreement with the experimental values as shown in Table 2. The  $R^2$  values in all cases tend towards unity ( $> 0.99$ ) showing a good fit of the data to the second order kinetic model. The initial swelling rate ( $R_i$ ) of the LBG-g-poly(DADMAC-co-AMPS) increases with pH up to 7.0 and later decreases as the pH is raised to 9.0. For LBG-g-poly(DADMAC-co-AMPS)/BNT, the  $R_i$  increases drastically acidic to basic medium. Isik and Sponza, (2004), reported a similar finding in respect of increase in  $R_i$ . But the swelling rate constant ( $k_2$ ) decreases as the pH values increases with respect to LBG-g-poly(DADMAC-co-AMPS). This is expected as the  $S_{eq}$  has an inverse relation with  $k_2$ . The value of  $k_2$  for LBG-g-poly(DADMAC-co-AMPS)/BNT also shows similar behavior.

Table 2: Kinetic data of Swelling for the terpolymer gel/composite

Swelling and kinetic parameters	LBG-g-poly(DADMAC-co-AMPS)			LBG-g-poly(DADMAC-co-AMPS)/BNT		
	pH 1.2	7.0	9.0	1.2	7.0	9.0
$S_{eq \text{ exp.}}$ (g/g)	5.70	7.09	7.16	5.95	16.52	8.42
$S_{eq \text{ cal.}}$ (g/g)	5.88	7.35	7.63	6.37	18.87	8.77
$k_2 \times 10^{-3}$ (g g <sup>-1</sup> min <sup>-1</sup> )	9.95	7.50	4.49	4.09	0.829	5.02
$R^2$	0.999	0.999	0.997	0.995	0.994	0.998
$R_i$ (min g <sup>-1</sup> g <sup>-1</sup> )	0.344	0.406	0.262	0.166	0.295	0.386

### 3.5. Dye adsorption studies

The adsorption study was carried out using indigo carmine (IC) as model dye. The structure of the dye molecule is given in Fig. 5.

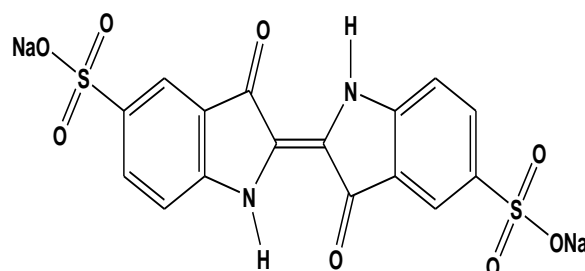


Fig. 5: Structure of Indigo carmine dye.

The effect of contact time on the adsorption capacity of LBG-g-poly(DADMAC-co-AMPS) and LBG-g-poly(DADMAC-co-AMPS)/BNT towards adsorption of IC is shown on Fig. 6. The amount of dye (mg/g) adsorbed increases linearly with time until equilibrium is reached. The equilibrium adsorption capacity of IC is found to be 17.36 and 11.99 mg/g respectively for LBG-g-poly(DADMAC-co-AMPS) and LBG-g-poly(DADMAC-co-AMPS)/BNT. The adsorption of IC on LBG-g-poly(DADMAC-co-AMPS) is attributed to the strong electrostatic interaction between the cationic ( $N^+$ ) group of the quaternary amino group of the grafted polymer and the anionic group ( $SO_3^-$ ) of the IC molecule.

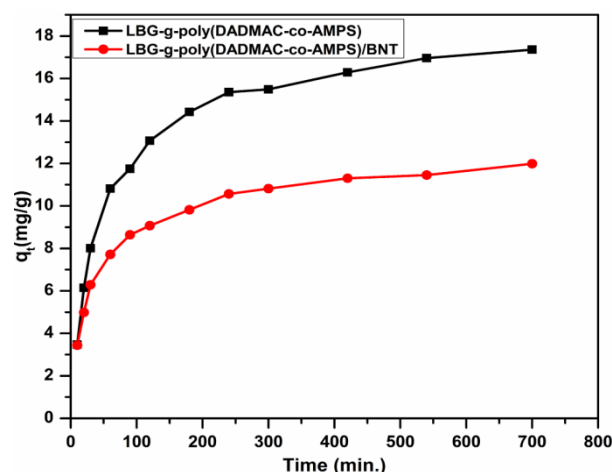


Fig. 6: Effect of contact time on the adsorption of IC dye (mg/g).

### 3.5.1. Adsorption isotherms

For equilibrium adsorption studies, fixed amount (0.05g) of the adsorbents were used in 25mL solution containing varied concentration of IC (10-100 mg/L) and the maximum amount of IC adsorbed in each case was determined. The three isotherm models namely; Freundlich (Freundlich and Heller, 1939), Langmuir (Langmuir, 1916) and Temkin (Temkin and Yakobson, 1984)

were employed in this work in order to understand the adsorption behavior of the dye on the adsorbents.

### 3.5.1.1. Freundlich isotherm

The Freundlich adsorption isotherm is based on the postulate that, the process of adsorption takes place on heterogeneous surfaces and the capacity of adsorption is related directly to the equilibrium concentration of the dye. The Freundlich isotherm is represented by the equation below;

$$\ln q_e = \ln k_f + \frac{1}{n} \ln C_e \quad (7)$$

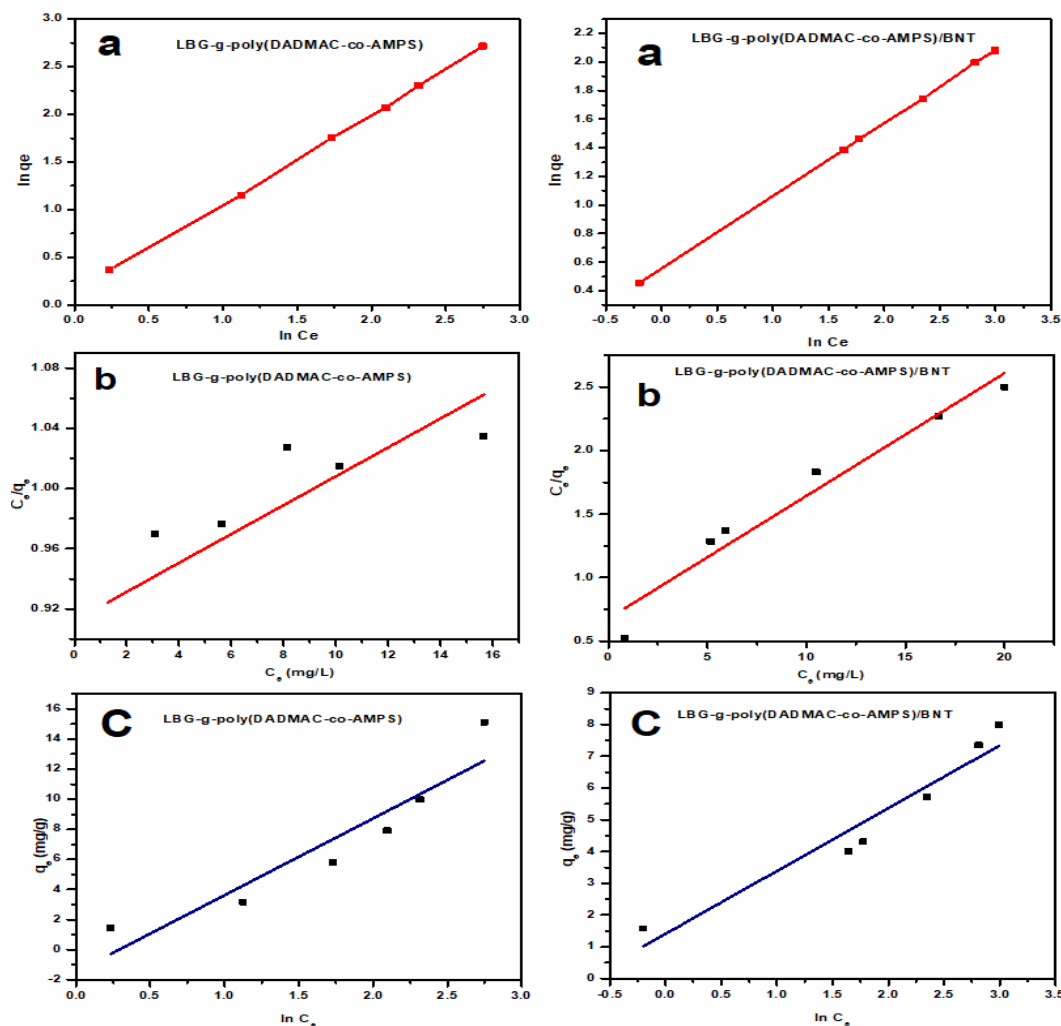


Fig. 7: a. Freundlich, b. Langmuir and c. Temkin isotherms for IC adsorption.

### 3.5.1.2. Langmuir model

The model that assumed the maximum adsorption corresponds to a saturated mono layer of solute molecules on the adsorbent surface is referred to as Langmuir adsorption model. It is expressed as eqn. 8 given below;

$$\frac{C_e}{q_e} = \frac{1}{q_m} \cdot C_e + \frac{1}{k_L q_m} \quad (8)$$

Where,  $C_e$ ,  $q_e$ ,  $q_m$  and  $k_L$  are the equilibrium concentration of dye (mg/L) solution, amount of dye adsorbed at equilibrium (mg/g), maximum adsorption corresponding to complete monolayer coverage on the surface (mg/g) and Langmuir constant which is related to the energy of adsorption (L/mg) respectively.  $k_L$  and  $q_m$  are determined from the intercept and slope of the linear plot of  $C_e/q_e$  versus  $C_e$  (Fig. 7b) and presented in table 3. The basic features of the Langmuir isotherm can be represented in terms of separation factor (dimensionless equilibrium parameter)  $R_L$  (Krušić, et al, 2012), which can be expressed as;

Where  $q_e$  is the amount of dye adsorbed at equilibrium (mg/g),  $C_e$  is the concentration of dye solution at equilibrium (mg/L),  $k_f$  and  $n$  are Freundlich adsorption isotherm constants that represent the extent of adsorption and the degree of nonlinearity between the dye concentration and the adsorption respectively. The values of  $k_f$  and  $n$  were calculated from the intercept and slope of the plot of  $\log q_e$  and  $\log C_e$  (Fig. 7a) and are presented in Table 3. The value of  $n$  indicates whether the adsorption is favorable or otherwise. If it lies within the range of 1 to 10 then, the adsorption is favorable. In this case, the adsorption of IC on LBG-g-poly(DADMAC-co-AMPS) and LBG-g-poly(DADMAC-co-AMPS)/BNT is considered to be favorable.

$$R_L = \frac{1}{1 + k_L C_0} \quad (9)$$

Where,  $C_0$  is the highest initial concentration of the dye (mg/L) and  $k_L$  is the Langmuir constant (L/mg). The value of  $R_L$  determined the nature of adsorption as indicated below;

- $R_L > 1$  Unfavorable adsorption
- $0 < R_L < 1$  Favorable adsorption
- $R_L = 0$  Irreversible adsorption
- $R_L = 1$  Linear adsorption

Hence, the values of  $R_L$  (Table 3) obtained in this study showed favorable adsorption of IC on LBG-g-poly(DADMAC-co-AMPS) and LBG-g-poly(DADMAC-co-AMPS)/BNT. The  $R^2$  values of Langmuir isotherm models are 0.68 and 0.96 respectively for LBG-g-poly(DADMAC-co-AMPS) and LBG-g-poly(DADMAC-co-AMPS)/BNT. This indicated that the equilibrium adsorption data is not well explained by the Langmuir model.

### 3.5.1.3. Temkin isotherm

The Temkin adsorption isotherm model is of the assumption that the free energy of sorption is a function of the surface coverage (Temkin and Yakobson, 1984). The Temkin isotherm is usually used for heterogeneous surface systems, ie non-uniform distribution of sorption (Erhayem, et al, 2015). The linear representation of the isotherm is;

$$q_e = B \ln K_T + B \ln C_e \quad (10)$$

Where  $C_e$  and  $q_e$  were defined as above;  $K_T$  is the equilibrium binding constant (L/g) and  $B$  is a constant related to the heat of sorption [J/mol]. The constants  $K_T$  and  $B$  were obtained from the slope of linear plot of  $q_e$  versus  $\ln C_e$  (Fig. 7c). From the Table 3, the  $R^2$  values obtained in both cases is low compared with Freundlich model. This shows that the adsorption of IC onto LBG-g-poly(DADMAC-co-AMPS) and LBG-g-poly(DADMAC-co-AMPS)/BNT cannot be explained by the Temkin model.

**Table 3:** Adsorption isotherms data for IC on Terpolymer gel/composite

Model	Parameters	Adsorbents	
		LBG-g-poly(DADMAC-co-AMPS)	LBG-g-poly(DADMAC-co-AMPS)/BNT
Freundlich	$n$	1.07	1.96
	$k_f$	1.14	0.917
	$R^2$	0.999	0.999
Langmuir	$q_{max}(\text{mg/g})$	111.11	10.42
	$R_L$	0.50	0.06
	$k_L(\text{L/mg})$	0.01	0.14
	$R^2$	0.68	0.96
	$K_T(\text{L/g})$	1.34	2.04
Temkin	$B(\text{J/Mol.})$	5.101	1.976
	$R^2$	0.88	0.94

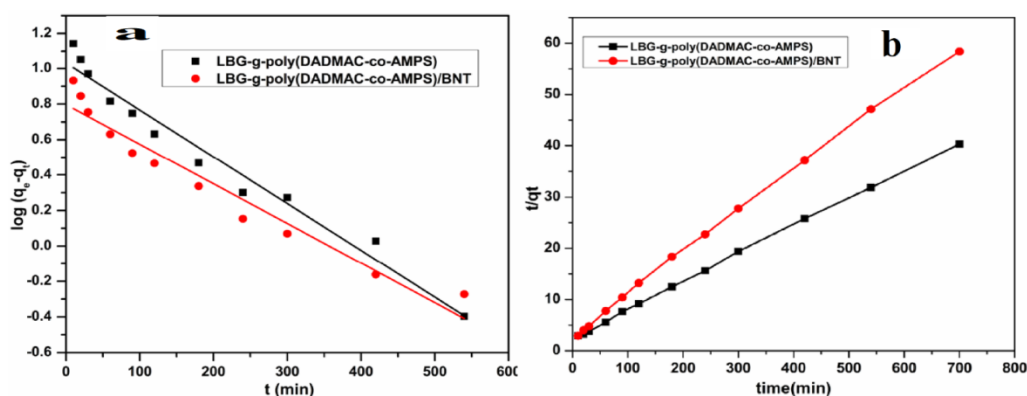


**Fig. 8:** Fit of Adsorption Kinetic Data: a. Pseudo First Order Model and b. Pseudo Second Order Model.

### 3.5.2.2. Pseudo second order kinetics

The pseudo second order kinetic equation (Ho and McKay, 1998) is expressed as:

$$\frac{t}{q_t} = \frac{1}{k_2 q_e^2} + \frac{1}{q_e} t \quad (12)$$

Where  $q_e$  and  $q_t$  are the values of dye adsorbed at equilibrium and at time  $t$  respectively (mg/g),  $k_2$  is the rate constant ( $\text{gmg}^{-1}\text{min}^{-1}$ ) for the pseudo-second order kinetic process and  $t$  is the time (min.) of adsorption. The plot of  $t/q_t$  vs  $t$  (Fig. 8b) gives a straight line from which it can be concluded that the adsorption is a pseudo second order kinetic process. The values of  $q_e$ ,  $k_2$  and  $R^2$  obtained from the intercept and slope of  $t/q_t$  vs  $t$  plot are presented in Table 4. The  $R^2$  values are 0.999 and 0.998 respectively for LBG-g-poly(DADMAC-co-AMPS) and LBG-g-poly(DADMAC-co-AMPS)/BNT. Furthermore, the values of  $q_{ecal}$  obtained from pseudo second order are in good agreement with the  $q_{eexp}$  when compared to pseudo first order kinetic model.

### 3.5.2. Adsorption kinetics

The adsorption kinetic models are used to examine the adsorption mechanism process. In this study the pseudo first and second order kinetics models proposed by Lagergren and Ho respectively were used to study the kinetics of IC adsorption on LBG-g-poly(DADMAC-co-AMPS) and LBG-g-poly(DADMAC-co-AMPS)/BNT.

#### 3.5.2.1. Pseudo first order kinetics

The Lagergren pseudo first order kinetic model is based on the assumption that the rate of change of adsorption of solute is directly proportional to the difference in equilibrium concentration and concentration over time (Karthika and Vishalakshi, 2015) and can be expressed as:

$$\log(q_e - q_t) = \log q_e - \frac{k_1}{2.303} t \quad (11)$$

Where  $q_e$  and  $q_t$  are the dye adsorption capacity at equilibrium and at time  $t$  respectively (mg/g),  $k_1$  is the rate constant ( $\text{min}^{-1}$ ) for the pseudo-first order kinetics and  $t$  is the time (min.) of adsorption. The rate constant ( $k_1$ ) and correlation coefficient were calculated from the plot of  $\log(q_e - q_t)$  versus  $t$  (Fig 8a) and tabulated in Table 4. It is observed from the data presented in Table 4 that there is no close agreement between the values of  $q_{ecal}$  and  $q_{eexp}$ . Also, the  $R^2$  (0.97 and 0.95) are lower when compared with the  $R^2$  values for the pseudo second order fit (0.999 and 0.998) for LBG-g-poly(DADMAC-co-AMPS) and LBG-g-poly(DADMAC-co-AMPS)/BNT respectively showing that the data does not fit well with the pseudo first order kinetic model.

**Table 4:** Adsorption kinetic data for IC on Terpolymer gel and the composite

Order	Parameters	Adsorbent	
		LBG-g-poly(DADMAC-co-AMPS)	LBG-g-poly(DADMAC-co-AMPS)/BNT
	$q_{eexp}(\text{mg/g})$	17.36	11.99
First	$q_{ecal}(\text{mg/g})$	10.72	6.27
	$k_1(\text{min}^{-1})$	0.005	0.005
	$R^2$	0.97	0.95
Second	$q_{ecal}(\text{mg/g})$	18.52	12.50
	$k_2(\text{gg}^{-1}\text{min}^{-1})$	0.001	0.002
	$R^2$	0.999	0.998

### 3.5.3. Comparison of adsorption of IC on to different adsorbents

The adsorption capacity of LBG-g-poly(DADMAC-co-AMPS) and LBG-g-poly(DADMAC-co-AMPS)/BNT towards IC dye was found to be 18.52 and 12.50 mg/g respectively and were compared with other adsorbents (Dalaran, et al, 2009; Jiwalak, et al, 2010,

Carvalho, et al, 2011; Dalaran, et al, 2011; Li, et al, 2012; Ramesh and Sreenivasa, 2015; Geyikçi, 2016; Zauro and Vishalakshi, 2016; Gopi, et al, 2017) and presented in Table 5. It could be observed that the adsorption capacity of LBG-g-poly(DADMAC-co-AMPS) and LBG-g-poly(DADMAC-co-AMPS)/BNT is significantly higher than some of the adsorbents (Jiwalak, et al, 2010; Carvalho, et al, 2011; Li et al, 2012; Ramesh and Sreenivasa, 2015; Gopi, et al, 2017), but is lower than few other materials (Dalaran, et al, 2009; Dalaran, et al, 2011; Zauro and Vishalakshi, 2016). Higher adsorption by LBG-g-PDADMAC compared to LBG-g-poly(DADMAC-co-AMPS) could be attributed to the incorporation of AMPS which reduces the adsorption due to repulsion between  $\text{SO}_3^-$  of the IC and the adsorbent. Similarly, DMAEMA-AMPS-HEMA/MMT showed higher affinity towards IC compared with LBG-g-poly(DADMAC-co-AMPS)/BNT. The grafting of the copolymer on the LBG and the nature of the clay (BNT) could be some of the factors responsible for the low adsorption.

**Table 5:** Kinetics data for adsorption of IC on Terpolymer gel and the composite

Adsorbent	$Q_e$ (mg/g)	Order	Reference
LBG-g-poly(DADMAC-co-AMPS)	18.52	2 <sup>nd</sup>	Present study
LBG-g-poly(DADMAC-co-AMPS)/BNT	12.50	2 <sup>nd</sup>	Present study
Zeolite fly ash	1.29	2 <sup>nd</sup>	Carvalho, et al, (2011)
Mg(OH) <sub>2</sub>	0.05	2 <sup>nd</sup>	Ramesh and Sreenivasa, (2015)
Silk	5.18	2 <sup>nd</sup>	Jiwalak, et al, (2010)
PVA/SiO <sub>2</sub> nanofiber	0.75	2 <sup>nd</sup>	Li et al, (2012)
MMT	18.41	1 <sup>st</sup>	Geyikçi (2016)
DMAEMA-AMPS-HEMA/MMT	125	2 <sup>nd</sup>	Dalaran, et al, (2009)
AA-DEAEMA/MMT	320	1 <sup>st</sup>	Dalaran, et al, (2011)
PVDF	12.5	-	Gopi, et al, (2017)
PVDF/ChNW	72.6	-	Gopi, et al, (2017)
LBG-g-PDADMAC	35.12	-	Zauro and Vishalakshi, (2016)

## 4. Conclusion

In this work a terpolymer gel consisting of LBG, DADMAC, AMPS and its composite with BNT clay were made via microwave irradiation. The terpolymer gel without clay component exhibited remarkably higher swelling at pH 7.0. The swelling kinetic studies suggested a second order swelling process under different pH conditions for both gel and its composite. The adsorption of IC on the terpolymer gel and the composite revealed that LBG-g-poly(DADMAC-co-AMPS) showed higher adsorption compared to LBG-g-poly(DADMAC-co-AMPS)/BNT. The decrease in adsorption of IC on LBG-g-poly(DADMAC-co-AMPS)/BNT could be attributed to acidic nature of both the IC and BNT clay which could result in electrostatic repulsion between the clay composite and the anionic dye. The adsorption data were observed to fit best into Freundlich model and the adsorption is found to follow second order kinetic model.

## Acknowledgements

One of the authors SAZ thanks the Government of India for providing the scholarship under the Indian Council for Cultural Relations (ICCR) and Usmanu Danfodiyo University, Sokoto, Nigeria for the study leave

## References

- [1] Bueno, V. B., Bentini, R., Catalani, L. H. and Petri, D. F. S. (2013). Synthesis and swelling behavior of xanthan based hydrogels, *Carbohydr. Polym.* 92: 1091–1099, <https://doi.org/10.1016/j.carbpol.2012.10.062>.
- [2] Carvalho, T. E. M. D., Fungaro, D. A., Magdalena, C. P., Cunico, P. (2011). Adsorption of indigo carmine from aqueous solution using coal fly ash and zeolite from fly ash, *J. Radioanal. Nucl. Chem.* 289: 617–626, <https://doi.org/10.1007/s10967-011-1125-8>.
- [3] Cestari, A. R., Vieira, E. F. S., Tavares, A. M. G. and Bruns, R. E. (2008). The removal of the indigo carmine dye from aqueous solutions using crosslinkedchitosan Evaluation of adsorption thermodynamics using a full factorial design, *J. Hazard. Mater.* 153: 566–574, <https://doi.org/10.1016/j.jhazmat.2007.08.092>.
- [4] Dalaran, M., Emik, S., Guclu, G., Iyim, T. B. and Ozgumus, S. (2009). Removal of acidic dye from aqueous solution using poly(DMAEMA-AMPS-HEMA) terpolymer/MMT nanocomposite hydrogels, *Polym. Bull.* 63: 159-171, <https://doi.org/10.1007/s00289-009-0077-4>.
- [5] Dalaran, M., Emik, S., Güçlü, G., İyim, T. B. and Özgümüş, S. (2011). Study on a novel polyampholytenanocomposite superabsorbent hydrogels: Synthesis, characterization and investigation of removal of indigo carmine from aqueous solution, *Desalin.* 279: 170–182, <https://doi.org/10.1016/j.desal.2011.06.004>.
- [6] Durmaz, S. and Okay, O. (2000). Acrylamide/2-acrylamido-2-methylpropane sulfonic acid sodium salt-based hydrogels: synthesis and characterization, *Polym.* 41(10): 3693–3704 [https://doi.org/10.1016/S0032-3861\(99\)00558-3](https://doi.org/10.1016/S0032-3861(99)00558-3).
- [7] El Haddad, M., Mamouni, R., Saffaj, N., Lazar, S. (2012). Adsorptive Removal of Basic Dye Rhodamine B from Aqueous Media onto Animal Bone Meal as New Low Cost Adsorbent, *Glob. J. Hum. Soc. Sci. Geog. & Environ. Geo-Sci.* 12: 19-29
- [8] Erhayem, M., Al-Tohami, F., Mohamed, R., Ahmida, K., (2015). Isotherm, kinetic and thermodynamic studies for the sorption of mercury (II) onto activated carbon from *Rosmarinus officinalis* leaves. *Am. J. Anal. Chem.*, 6: 1-10, <https://doi.org/10.4236/ajac.2015.61001>.
- [9] Fosso-kankeu, E., Mittal, H., Mishra, S. B. and Mishra, A. K. (2015). Gum ghatti and acrylic acid based biodegradable hydrogels for the effective adsorption of cationic dyes. *J. Ind. Eng. Chem.* 22: 171.178, <https://doi.org/10.1016/j.jiec.2014.07.007>.
- [10] Gan, L., Shang, S., Hu, E., Yuen, C. W. M. and Jiang, S. (2015). KonjacGlucomannan/grapheme oxide hydrogels with enhance dye adsorption capability for methyl blue and methyl orange. *Appl. Sur. Sci.* 357: 866-872, <https://doi.org/10.1016/j.apsusc.2015.09.106>.
- [11] Ganji, F., Vasheghani-Farahani, S., and Vasheghani-Farahani, E. (2010). Theoretical Description of Hydrogel Swelling: A Review, *Iran. Polym. J.* 19(5): 375-398.
- [12] Geyikçi, F. (2016). Factorial design analysis for adsorption of Indigo Carmine onto Montmorillonite: Evaluation of the kinetics and equilibrium, *Prog. Org. Coatings* 98: 28-34, <https://doi.org/10.1016/j.porgcoat.2016.04.019>.
- [13] Giri, T. K., Pure, S. and Tripath, D. K. (2015). Synthesis of Graft Copolymer of Acrylamide for Locust Bean Gum using Microwave Energy: Swelling Behaviour, Flocculation Characteristic and Acute Toxicity Study. *Polimeros*, 25(2): 168-174, <https://doi.org/10.1590/0104-1428.1717>.
- [14] Gopi, S., Balakrishnan, P., Piusa, A. and Thomas, S. (2017). Chitin nanowhisker (ChNW) functionalized electrospun PVDF membrane for enhanced removal of Indigo carmine, *Carbohydr. Polym.* 165: 115–122, <https://doi.org/10.1016/j.carbpol.2017.02.046>.
- [15] Gupta, S. K., Nayunigari, M. K., Misra, R., Ansari, F. A., Dionysiou, D. D., Maity, A., Bux, F. (2016). Synthesis and Performance Evaluation of a New Polymeric Composite for the Treatment of Textile Wastewater, *Ind. Eng. Chem. Res.*, 55: 3–20, <https://doi.org/10.1021/acs.iecr.5b03714>.
- [16] Freundlich, H. and Heller, W. (1939). The Adsorption of cis and trans-Azobenzene, *J. Am. Chem. Soc.*, 61(8):228-230, <https://doi.org/10.1021/ja01877a071>.
- [17] Ho, Y. S. and McKay, G. (1998). A Comparison of Chemisorptions Kinetics Models Applied to Pollutant Removal of Various Sorbents. *Trans IchemE*, 76 Part B: 332-340 <https://doi.org/10.1205/095758298529696>.
- [18] İsiğ, M and Sponza D. T. (2004). Anaerobic/aerobic sequential treatment of a cotton textile mill wastewater, *J. Chem. Technol. Biotechnol.* 79(11): 1268–1274, <https://doi.org/10.1002/jctb.1122>.
- [19] Jing, R. and Hongfei, H. (2001). Study of Interpenetrating Polymer Network Hydrogels of Diallyldimethylammonium Chloride with Kappa-Carrageenan by UV Irradiation. *Eur. Polym. J.* 37: 2413-2417, [https://doi.org/10.1016/S0014-3057\(01\)00146-X](https://doi.org/10.1016/S0014-3057(01)00146-X).
- [20] Jiwalak, N., Rattanaphani, S., Bremner, J. B. and Rattanaphani, V. (2010). Equilibrium and Kinetic Modeling of the Adsorption of In-

- digo Carmine onto Silk, *Fibers and Polym.*, 11(4): 572-579, <https://doi.org/10.1007/s12221-010-0572-2>.
- [21] Kaity, S., Isaac, J., Kumar, P. M., Bose, A., Wong, T. W. and Ghosh, A. (2013). Microwaveassisted synthesis of acrylamide grafted locust bean gum and its application in drug delivery, *Carbohydr. Polym.* 98(1): 1083–1094, <https://doi.org/10.1016/j.carbpol.2013.07.037>.
- [22] Karthika, J. S. and Vishalakshi, B. (2015). Novel stimuli responsive gellan gum-graft-poly(DMAEMA) hydrogel as adsorbent for anionic dye. *Int. J. Biol. Macromol.* 81: 544-655, <https://doi.org/10.1016/j.ijbiomac.2015.08.064>.
- [23] Krušić, M. K., Milosavljević, N., Debeljković, A., Ūzüm, Ö. B. and Karadağ, E. (2012). Removal of Pb<sup>2+</sup> Ions from Water by Poly(Acrylamide-co-Sodium Methacrylate) Hydrogels. *Water, Air, Soil Pollut.* 223: 4355-4368, <https://doi.org/10.1007/s11270-012-1200-y>.
- [24] Langmuir, I., (1916). The constitution and fundamental properties of solids and liquids, *J. Am. Chem. Soc.*, 38 (11): 2221–2295, <https://doi.org/10.1021/ja02268a002>.
- [25] Li, M., Wang, H., Wu, S., Li, F. and Zhi, P. (2012). Adsorption of hazardous dyes indigo carmine and acid red on nanofiber Membranes, *RSC Adv.* 2: 900–907, <https://doi.org/10.1039/C1RA00546D>.
- [26] Mahida, V. P., Patel, M. P. (2016). Superabsorbent amphoteric nanohydrogels: Synthesis, characterization and dyes adsorption studies, *Chin. Chem. Lett.* 27: 471–474, <https://doi.org/10.1016/j.ccllet.2015.12.015>.
- [27] Maity, J., Ray, S. K. (2016). Enhanced adsorption of Cr(VI) from water by guar gum based composite hydrogels, *Int. J. Biol. Macromol.* 89: 246-255, <https://doi.org/10.1016/j.ijbiomac.2016.04.036>.
- [28] Malana, M. A., Ijaz, S. and Ashiq, M. N. (2010). Removal of various dyes from aqueous media onto polymeric gel by adsorption process: their kinetics and thermodynamics. *Desalin.* 263:249-257, <https://doi.org/10.1016/j.desal.2010.06.066>.
- [29] Martínez-Ruvalcaba, A., Sánchez-Díaz, J. C., Becerra, F., Cruz-Barba, L. E. and González-Álvarez, A. (2009). Swelling characterization and drug delivery kinetics of polyacrylamide-co-itaconic acid/chitosan hydrogels, *eXPRESS Polym. Lett.* 3(1): 25–32, <https://doi.org/10.3144/expresspolymlett.2009.5>.
- [30] Mithun, U and Vishalakshi, B. (2014). Swelling Kinetics of a pH Sensitive Polyelectrolyte Complex of Polyacrylamide-g-alginate and Chitosan, *Int. J. Chemtech Res.* 6(7): 3579-3588
- [31] Patil, M. R., Shrivastava, V. S. (2015). Adsorption removal of carcinogenic acid violet19 dye from aqueous solution by polyaniline-Fe<sub>2</sub>O<sub>3</sub> magnetic nano-composite, *J. Mater. Environ. Sci.* 6:11-21
- [32] Ramesh, T. N. and Sreenivasa, V. P. (2015). Removal of Indigo Carmine Dye from Aqueous Solution using Magnesium Hydroxide as an Adsorbent, *J. Mater.* 2015: 1-10, <https://doi.org/10.1155/2015/753057>.
- [33] Robati, D., Mirza, B., Ghazisaeidi, R., Rajabi, M., Moradi, O., Tyagi, I., Agarwal, S., Gupta, V. K. (2016). Adsorption behavior of methylene blue dye on nanocomposite multi-walled carbon nanotube functionalized thiol (MWCNT-SH) as new adsorbent, *J. Mol. Liq.* 216: 830–835, <https://doi.org/10.1016/j.molliq.2016.02.004>.
- [34] Santos, S. C. R., Boaventura, R. A. R. (2016). Adsorption of cationic and anionic azo dyes on sepiolite clay: Equilibrium and kinetic studies in batch model, *J. Environ. Chem. Eng.* 4: 1473–1483, <https://doi.org/10.1016/j.jece.2016.02.009>.
- [35] Sebastian, S., Mayadevi, S., Beevi, B. S., Mandal, S. (2014). Layered Clay-Alginate Composites for the Adsorption of Anionic Dyes: A Biocompatible Solution for Water/Wastewater Treatment, *J. Water Res. Prot.* 6, 177-184, <https://doi.org/10.4236/jwarp.2014.63023>.
- [36] Shukla, N.B., Rattan, S and Madras, G. (2012). Swelling and Dye adsorption Characteristics of Amphoteric Superadsorbent Polymer, *Ind. Eng. Chem. Res.* 51: 14941-14948, <https://doi.org/10.1021/ie301839z>.
- [37] Temkin, S. I. and Yakobson, B. I. (1984). Diffusion-controlled reactions of chemically anisotropic molecules, *J. Phys. Chem.*, 88(13): 2679–2682, <https://doi.org/10.1021/j150657a001>.
- [38] Tirelli, N and Hunkeler, D. J. (1999). Variation in the Diallyldimethylammonium Chloride (DADMAC) Polymers Architectures: PEG/DADMAC blocks and Partially Quaternarised Polymers. *Macromol. Chem. Phys.*, 200 (5): 1068-1073, DOI: 10.1002/(SICI)1521-393
- [39] Zauro, S. A. and Vishalakshi, B. (2016). Microwave Assisted Synthesis of Poly(Diallyldimethylammonium Chloride) Grafted Locust Bean Gum: Swelling and Dye Adsorption Studies, *Indian J. Adv. Chem. Sci.* S1: 88-91
- [40] Zhao, Q., Sun, J., Chen, S and Zhou, Q. (2010). Properties of Poly(Acrylamide-co-diallyldimethylammonium Chloride) Hydrogels Synthesised in a Water-Ionic liquid Binary System. *J. Appl. Polym. Sci.* 115(5): 2940-2945, <https://doi.org/10.1002/app.31368>.
- [41] Zhou, C., Wu, Q., Lei, T and Negulescu, I. I. (2014). Adsorption kinetic and equilibrium studies for methylene blue dye by partially hydrolysed polyacrylamide/cellulose nanocrystal nano composite hydrogels. *Chem. Eng. J.* 251: 17-24, <https://doi.org/10.1016/j.cej.2014.04.034>.